

Dynamics of a rod in a homogeneous/inhomogeneous frozen disordered medium: Correlation functions and non-Gaussian effects

Angel J. Moreno^{1,2} and Walter Kob³

¹*Laboratoire des Verres. Université Montpellier 2. Place E. Bataillon. CC 069. F-34095 Montpellier, France.*

²*Present address: Donostia International Physics Center, Paseo Manuel de Lardizabal 4, E-20018 San Sebastián, Spain.*

³*Laboratoire des Colloïdes, Verres et Nanomatériaux, Université Montpellier 2, F-34095 Montpellier, France*

We present molecular dynamics simulations of the motion of a single rigid rod in a disordered static 2d-array of disk-like obstacles. Two different configurations have been used for the latter: A completely random one, and which thus has an inhomogeneous structure, and an homogeneous “glassy” one, obtained from freezing a liquid of soft disks in equilibrium. Small differences are observed between both structures for the translational dynamics of the rod center-of-mass. In contrast to this, the rotational dynamics in the glassy host medium is strongly slowed down in comparison with the random one. We calculate angular correlation functions for a wide range of rod length L and density of obstacles ρ as control parameters. A two-step decay is observed for large values of L and ρ , in analogy with supercooled liquids at temperature close to the glass transition. In agreement with the prediction of the Mode Coupling Theory, a time-length and time-density scaling is obtained. In order to get insight on the relation between the heterogeneity of the dynamics and the structure of the host medium, we determine the deviations from Gaussianity at different length scales. Strong deviations are obtained even at spatial scales much larger than the rod length. The magnitude of these deviations is independent of the nature of the host medium. This result suggests that the large scale translational dynamics of the rod is affected only weakly by the presence of inhomogeneities in the host medium.

Ref.: AIP Conference Proceedings 708 (2004) 576-582

I. INTRODUCTION

Since it was initially introduced by Lorentz as a model for the electrical conductivity in metals [1], the problem of the Lorentz gas has given rise to a substantial theoretical effort aimed to understand its properties [2, 3, 4, 5, 6, 7, 8]. In this model, a *single* classical particle moves through a disordered array of *static* obstacles. It can thus be used as a simplified picture of the motion of a light atom in a disordered environment of heavy particles having a much slower dynamics. In the simplest case, where the diffusing particle and the obstacles are modeled as hard spheres, an exact solution for the diffusion constant exists in the limit of low densities of obstacles [9]. However, the problem becomes highly non-trivial with increasing density, where dynamic correlations and memory effects start to become important for the motion of the diffusing particle, and the system shows the typical features of the dynamics of supercooled liquids or dense colloidal systems, such as a transition to a non-ergodic phase of zero diffusivity [2, 3, 4, 6]. In particular, diffusion constants and correlation functions are non-analytical functions of the density [2, 4, 7, 8]. Moreover, correlation functions show non-exponential long-time decays.

Diffusing particles and obstacles are generally modeled as disks or spheres in two and three dimensions, respectively. Much less attention has been paid to systems that have orientational degrees of freedom. Motivated by this latter question, we have recently started an investigation, at low and moderate densities of obstacles, on a generalization of the Lorentz gas, namely a model in which the diffusing particle is a rigid rod [10]. An array of randomly

distributed disks has been used for the host medium. For simplicity simulations have been done in two dimensions, reducing the degrees of freedom to the center-of-mass position and the orientation of the rod axis. As in the case of supercooled liquids [11, 12, 13, 14, 15] or dense colloidal systems [16, 17, 18], one observes at intermediate times a caging regime for the rod center-of-mass motion, which is due to the steric hindrance produced by the presence of the neighboring obstacles.

More interestingly, strong deviations from Gaussianity have been obtained for the incoherent intermediate scattering function at wavelengths much longer than the rod length, giving evidence for a strongly heterogeneous character of the long-time dynamics at such length scales. The inhomogeneous structure of the model used for the host medium has been pointed out as a possible origin of such non-Gaussian effects since a random configuration features large holes on one side but on the other side also dense clusters of obstacles. The presence of holes might lead to a finite probability of jumps that are much longer than the average “jump length” and thus to a heterogeneous dynamics.

In order to shed new light on this question, we have repeated the simulations by taking a disordered but *homogeneous* configuration of the obstacles instead of a random one. We will see, however, that large scale non-Gaussian effects are not significantly affected by the particular choice of the configuration of the obstacles. Some information on angular correlation functions is also presented. The article is organized as follows: In Section II we present the model and give details of the simulation. Translational and angular mean-squared displacements are presented in Section III. The behavior of angular cor-

relation functions is shown and discussed in Section IV, in terms of the Mode Coupling Theory. Non-Gaussian effects in the random and glassy models of the host medium are investigated in Section V. Conclusions are given in Section VI.

II. MODEL AND DETAILS OF THE SIMULATION

The rigid rod, of mass M , was modeled as N aligned point particles of equal mass $m = M/N$, with a bond length 2σ . The rod length is therefore given by $L = (2N - 1)\sigma$. The positions of the obstacles in the random configuration were generated by a standard Poisson process. In order to obtain the glassy host medium, we equilibrated at a reduced particle density $\rho = 0.77$ and at temperature $T = \epsilon/k_B$ a two-dimensional array of point particles interacting via a soft-disk potential $V(r) = \epsilon(\sigma/r)^{12}$. This procedure produced an homogeneous liquid-like configuration. The latter was then permanently frozen and was expanded or shrunk to obtain the desired density of obstacles, defined as $\rho = n_{\text{obs}}/l_{\text{box}}^2$, with n_{obs} the number of obstacles and l_{box} the length of the square simulation box used for periodic boundary conditions.

The same soft-disk potential $V(r)$ was used for the interaction between the particles forming the rod and the obstacles. For computational efficiency, $V(r)$ was truncated and shifted at a cutoff distance of 2.5σ . In the following, space and time will be measured in the reduced units σ and $(\sigma^2 m/\epsilon)^{1/2}$, respectively. Typically 600-1000 realizations of the ensemble rod-obstacles were considered. The set of rods was equilibrated at $T = \epsilon/k_B$. After the equilibration, a production run was done at constant energy and results were averaged over the different realizations. These runs covered 10^6 time units, corresponding to $(1-5) \cdot 10^8$ time steps, depending on the step size used for the different rod lengths and densities. Run times were significantly longer than the relaxation times of the system.

III. MEAN-SQUARED DISPLACEMENTS

Figs. 1a and 1b show respectively for $\rho = 6 \cdot 10^{-3}$ a comparison between the random and the glassy configuration for the mean-squared displacement of the rod center-of-mass $\langle(\Delta r(t))^2\rangle$ and the mean-squared angular displacement $\langle(\Delta\Phi(t))^2\rangle$. Brackets denote ensemble average. In order to facilitate the observation of the different dynamic regimes, data have been divided by the time t . The comparison covers a wide range of rod lengths from $L \sim 0.1d_{\text{nn}}$ to $L \sim 10d_{\text{nn}}$, where $d_{\text{nn}} = \rho^{-1/2} \approx 13$, is the average distance between obstacles for the mentioned density. At short times the rod does not feel the presence of the neighboring obstacles and $\langle(\Delta r(t))^2\rangle$ and $\langle(\Delta\Phi(t))^2\rangle$ show the quadratic time-dependence characteristic of a ballistic motion. For the shortest rods a sharp transition to the long-time linear regime is observed. In contrast to this, for long rods a crossover regime between both limits, showing a weaker time dependence that the

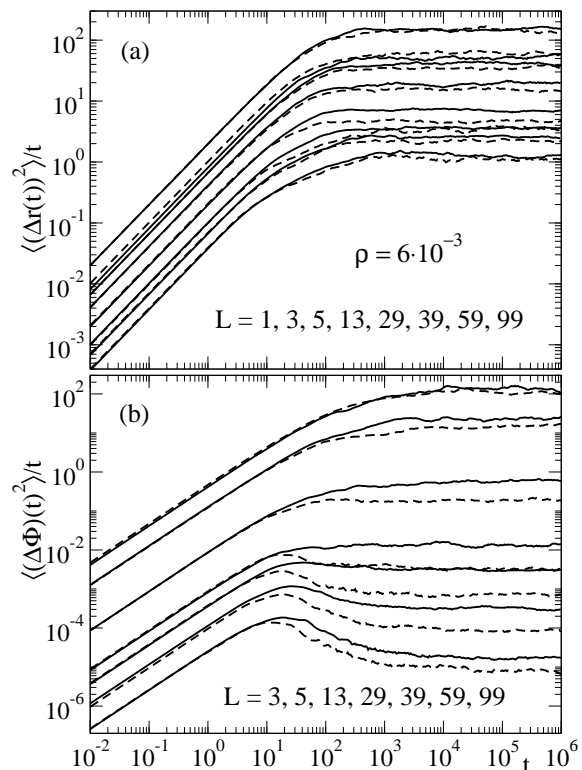


FIG. 1: Mean-squared displacement of the center-of-mass (a) and mean-squared angular displacement (b), both divided by the time t , for $\rho = 6 \cdot 10^{-3}$ and different rod lengths, for the random (solid lines) and glassy (dashed lines) configuration of the obstacles.

ballistic motion, is present over 1-2 decades of intermediate times. Such a crossover corresponds to the well-known caging regime [11, 12, 13, 14, 15, 16, 17, 18] observed in supercooled liquids or dense colloidal systems. Due to the presence of the neighboring obstacles, the particle is trapped within an “effective cage” for some time until it escapes from it and begins to show a diffusive behavior.

No significant differences are observed between the values of $\langle(\Delta r(t))^2\rangle$ for a same rod length in the two different, random and glassy, configurations. This is more clearly seen by calculating for each L the ratio $D_{\text{CM}}^{\text{ran}}/D_{\text{CM}}^{\text{gla}}$ between the center-of-mass translational diffusion constant D_{CM} in both configurations. The latter is calculated as the long-time limit of $\langle(\Delta r(t))^2\rangle/4t$. As shown in Fig. 2, differences in D_{CM} between the random and the glassy host medium are less than a factor 1.5. The values of D_{CM} are systematically lower for the glassy host medium, evidencing a stronger backscattering for the diffusion, as intuitively expected from the homogeneous character of this latter configuration in contrast to the random one (see Fig. 3), where the presence of holes facilitates diffusion. It is noteworthy that the maximum difference between the values of D_{CM} in both configurations takes place for $L \sim 10 - 20$, i.e., when the rod becomes longer than d_{nn} . Thus, while in the homogeneous glassy host medium the rod will not be able to pass transversally between two neighboring obstacles, in the inhomogeneous random configuration this diffusion channel will still be present due to the presence of holes

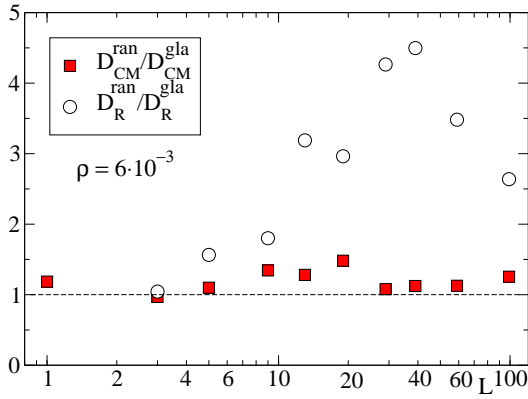


FIG. 2: Ratio between the rotational and center-of-mass translational diffusion constants for the random and the glassy host medium at $\rho = 6 \cdot 10^{-3}$ and different rod lengths.

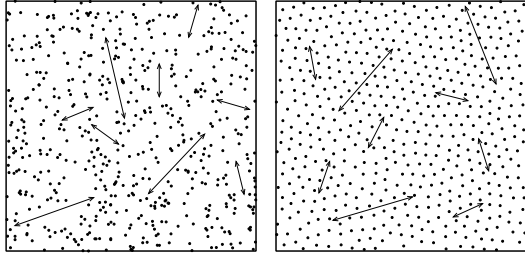


FIG. 3: Two configurations of the obstacles for a same density $\rho = 6 \cdot 10^{-3}$. Left: A random configuration. Right: A homogeneous glassy configuration. Short and long arrows correspond, respectively, to distances of 40 and 100.

and will only be suppressed for very long rods.

Strong differences are observed between both models of the host medium in the case of the rotational dynamics, as shown in Fig. 1b for $\langle(\Delta\Phi(t))^2\rangle$ and in Fig. 2 for the ratio of the rotational diffusion constants, $D_R^{\text{ran}}/D_R^{\text{gla}}$. (D_R is calculated as the long-time limit of $\langle(\Delta\Phi(t))^2\rangle/2t$.) For rod lengths smaller than d_{nn} the rotational dynamics is only weakly sensitive to the configuration of the medium and the ratio $D_R^{\text{ran}}/D_R^{\text{gla}}$ remains close to unity. However, for rods longer than d_{nn} the latter ratio strongly increases up to a maximum of ~ 4.5 for $L \sim 40$. The position of the maximum can be again rationalized from the inhomogeneous structure of the random host medium. Short arrows in the configurations of Fig. 3 for $\rho = 6 \cdot 10^{-3}$ indicate distances of 40. From the comparison between both configurations it is clear that while in the glassy medium rods of $L \sim 40$ can perform only small rotations within the tubes formed by the neighboring obstacles, in the random medium they can go into the holes and thus rotate freely over a larger angle. Therefore, the long-time angular displacement will grow up more quickly than for the motion between narrow tubes in the glassy configuration. It must also be mentioned

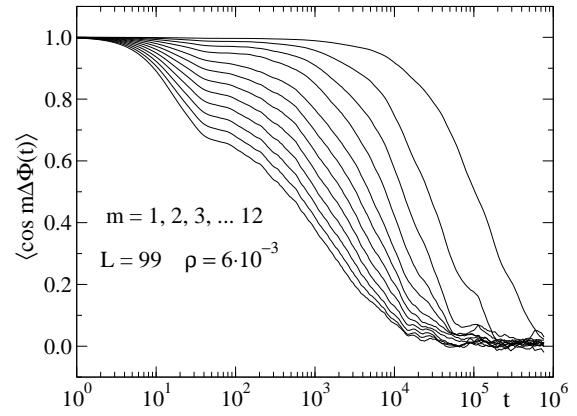


FIG. 4: Correlation function $\langle\cos m\Delta\Phi(t)\rangle$ for $L = 99$ and $\rho = 6 \cdot 10^{-3}$, with $m = 1, 2, 3, \dots, 12$ (from top to bottom). Data correspond to the random host medium.

that even for the largest investigated rod length, $L = 99$, where motion between tubes also dominates the diffusion in the random medium, the ratio $D_R^{\text{ran}}/D_R^{\text{gla}}$ is still significantly different from unity. Thus, while in the glassy medium the walls of the tube are formed by uniformly distributed obstacles, in the random configuration long distances are allowed between some of the neighboring obstacles forming the tube, leading to additional escaping channels (see long arrows in Fig. 3). In principle, only for extremely long rods the ratio $D_R^{\text{ran}}/D_R^{\text{gla}}$ is expected to approach unity.

IV. CORRELATION FUNCTIONS

The Mode Coupling Theory (MCT) [19, 20, 21, 22] makes precise quantitative predictions on the dynamics of supercooled liquids or dense colloidal systems. In its idealized version, it predicts a dynamic transition from an ergodic to a non-ergodic phase at some critical value of the control parameters. These are usually the temperature or the density, though in principle the MCT formalism can be generalized to other control parameters. Moreover, it has been recently tested in a kind of systems very different from liquids or colloids, such as plastic crystals [23], suggesting a more universal character for this theory. Motivated by this possibilities, we test some predictions of MCT for the rotational dynamics of the rod with L and ρ as control parameters.

According to MCT, upon approaching the critical point, the correlation function shows a two-step decay. The initial decay corresponds to the dynamic transition from the ballistic to the caging regime. As a consequence of the temporary trapping in the cage formed by the neighboring obstacles, the particle does not lose the memory of its initial position and the correlation functions decay very slowly, giving rise to a plateau at intermediate times between the ballistic and the diffusive regime. The dynamics close to this plateau is usually referred as the β -relaxation. The closer the control parameters are to the critical values, the slower is the mobility of the particles and the longer is the lifetime of the cage, leading

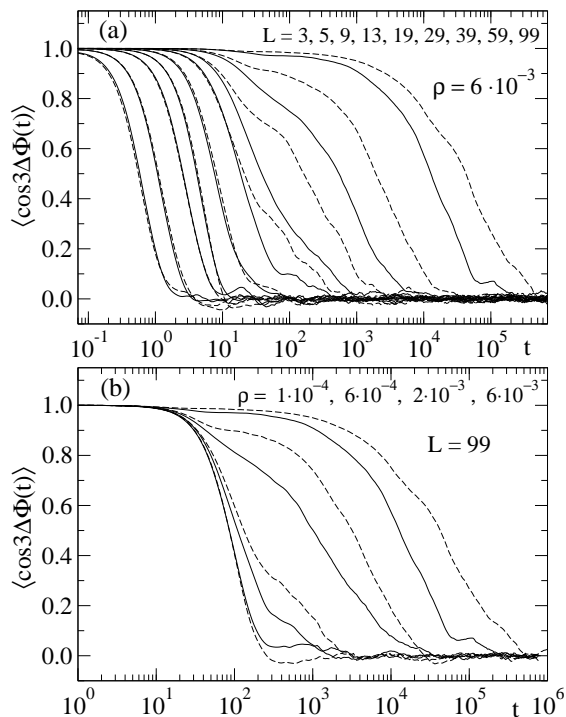


FIG. 5: (a) Correlation function $\langle \cos 3\Delta\Phi(t) \rangle$ for $\rho = 6 \cdot 10^{-3}$ and different rod lengths; (b) The same function for $L = 99$ and different densities. Solid and dashed lines correspond, respectively, to the random and the glassy configurations of the host medium.

to a longer plateau in the correlation function. Finally, at much longer times, the particle escapes from the cage and loses memory of its initial environment, leading to a second long-time decay of the correlation function to zero, known as the α -relaxation.

Fig. 4 shows the behavior of the angular correlators $\langle \cos m\Delta\Phi(t) \rangle$ for $m = 1, 2, 3, \dots, 12$ for a density of obstacles $\rho = 6 \cdot 10^{-3}$ and a rod length $L = 99$ much longer than d_{nn} . Data are shown for the random host medium, though for the glassy one they show the same qualitative behavior. Though it is difficult to see it for the smallest values of m , the plateau is clearly visible for $m \geq 4$. Thus, long rods will only perform small rotations before hitting the walls of the tube. As a consequence, the correlators for small m will decrease only very weakly during the ballistic regime, and hence it will be difficult to see the subsequent plateau. In contrast to this, for higher-order correlators, the angle rotated during the ballistic regime will be amplified by a factor m , leading to a stronger decay before the caging regime and facilitating the observation of the plateau. The latter begins to develop around $t \sim 30$. As can be seen in Fig. 1b for the curve for $L = 99$, this time corresponds to the beginning of the caging regime for the mean-squared angular displacement, in agreement with the MCT prediction.

Fig. 5 shows for $m = 3$, and for the two models of host medium, how the plateau develops with increasing rod length and density of obstacles. While for values of L below d_{nn} , the correlators show a simple decay and within the error bar show no difference between both models of the host medium, a clear difference is observed for longer

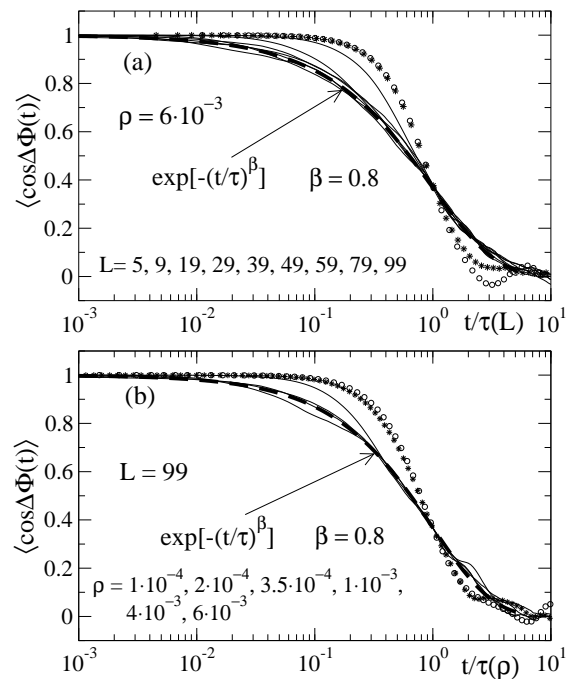


FIG. 6: (a) Time-length superposition for $\langle \cos \Delta\Phi(t) \rangle$ at density $\rho = 6 \cdot 10^{-3}$; (b) Time-density scaling for the same function for length $L = 99$. For the sake of clarity the lowest values of ρ and L have been represented with points. Dashed lines are fits to KWW functions. The stretching exponents are indicated in the figure. Data correspond to the random host medium.

rods. Thus, for the glassy medium rotational relaxation times become about a decade larger and the plateau is significantly higher than in the random configuration, in agreement with the results presented in Section III for the mean-squared angular displacement.

Another important prediction of the MCT is the so called “second universality”: given a correlator $g(t, \zeta)$, with ζ a control parameter, then one has that, in the time scale of the α -regime, the correlator follows a scaling law $g(t, \zeta) = \tilde{g}(t/\tau(\zeta))$, where $\tau(\zeta)$ is the ζ -dependence of the relaxation time τ of the α -regime for such a correlator, and \tilde{g} is a master function. The relaxation time is in practice defined as the time where the correlator decays to an arbitrary but small fraction of its initial value, or is obtained from fitting the α -decay of the correlator to a Kohlrausch-Williams-Watts (KWW) function, $\exp(-(t/\tau)^\beta)$, widely used in the analysis of relaxations in complex systems [24]. In most of the experimental situations the relevant control parameter is the temperature and for that reason, the second universality is often referred as the “time-temperature superposition principle”. Now we test the existence of a time-length and a time-density superposition principle for the angular correlators of the rod. Fig. 6 shows the correlators $\langle \cos \Delta\Phi(t) \rangle$ as a function of the scaled times $t/\tau(L)$ for constant density $\rho = 6 \cdot 10^{-3}$, and $t/\tau(\rho)$ for constant rod length $L = 99$. Data are shown for the random host medium. The relaxation times τ have been defined as $\langle \cos \Delta\Phi(\tau) \rangle = 1/e$. Apart from the trivial scaling in the limit of short rods and low densities, a good superposition to a master curve is obtained for larger values of L and ρ , confirming the

second universality of the MCT for this system. The master curve can be well reproduced by a KWW function with a stretching exponent $\beta = 0.8$, as shown in Fig. 6. Analogous results, with a very similar stretching exponent, are obtained for the glassy host medium.

V. NON-GAUSSIAN EFFECTS

In Einstein's random walk model for diffusion, particles move under the effect of collisions with the others. When a particle undergoes a collision, it changes its direction randomly, and completely loses the memory of its previous history. When the time and spatial observational scales are much larger than the characteristic time and the mean free path between collisions, the van Hove self-correlation function, i.e., the time and spatial probability distribution $G_s(r, t)$ of a particle initially located at the origin, is given by a Gaussian function [25]. This functional form is exact for an ideal gas and for an harmonic crystal. It is also valid in the limit of short times, where atoms behave as free particles. When the system is observed at time and length scales comparable to those characteristic of the collisions, the possible intrinsic dynamic heterogeneities of the system will be reflected by strong deviations from Gaussianity in $G_s(r, t)$. Such deviations are usually quantified by the so-called second-order non-Gaussian parameter $\alpha_2(t)$, which in two-dimensions is defined as $\alpha_2(t) = [\langle (\Delta r(t))^4 \rangle / 2 \langle (\Delta r(t))^2 \rangle^2] - 1$. For a Gaussian function in two dimensions, $\alpha_2(t) = 0$, while deviations from Gaussianity result in finite values of $\alpha_2(t)$.

Our previous investigation [10] on the non-Gaussian parameter in the random host medium revealed some features similar to those observed in supercooled liquids or dense colloids, such as the development of a peak (see also Fig. 7), which grows with increasing rod length - in analogy to decreasing temperature in supercooled liquids or increasing density in colloids. As also observed in these latter systems [11, 12, 13, 14, 15, 16, 17, 18], the region around the maximum of the peak corresponds to the time interval corresponding to the end of the caging and the beginning of the long-time diffusive regime. Thus, the breaking of the cage leads to a finite probability of jumps much longer than the size of the cage, resulting in a strongly heterogeneous dynamics at that intermediate time and spatial scale, which is reflected by a peak in the non-Gaussian parameter.

Another interesting result was the observation that, in particular for long rods, in the time span of the simulation, i.e. for time scales that are much longer than the typical relaxation time of the system, $\alpha_2(t)$ did not decay to zero but remained finite [10]. Thus, the long-time dynamics is still significantly non-Gaussian, i.e. heterogeneous, at the spatial scale - much larger than the rod length- covered by the simulation. In order to investigate the possibility of a relation of this large-scale non-Gaussian dynamics with the presence of holes in the random structure of obstacles, that might lead to a finite probability of jumps much longer than the average, as pointed out in Ref.[10], we have calculated $\alpha_2(t)$ for the

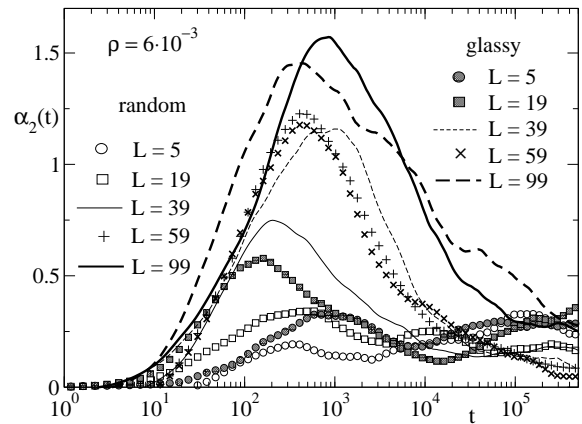


FIG. 7: Time-dependence of the non-Gaussian parameter $\alpha_2(t)$ for different values of L and for the random and the glassy host medium at density $\rho = 6 \cdot 10^{-3}$.

dynamics of the rod in the glassy host medium. Fig. 7 shows a comparison between the non-Gaussian parameter in both structures for several rod lengths and density $\rho = 6 \cdot 10^{-3}$. While in the limit of short and long rods $\alpha_2(t)$ takes similar values for both configurations in all the time window investigated, a much more pronounced peak is observed at intermediate rod lengths for the glassy configuration. This result can be rationalized by the absence of holes in the homogeneous glassy host medium. Thus in the latter, jumps that lead to an escape from the cage formed by the neighboring obstacles will be necessarily long, since long rods will be confined in tubes which they will be able to leave only by making a long longitudinal motion. In contrast to this, the above mentioned inhomogeneous nature of the tube walls in the random structure will allow the rod to escape the cage also by shorter jumps, resulting in a less heterogeneous caging regime. Only rods much longer than the hole size will need long jumps to escape from the tubes in the random host medium and the caging regime will become as heterogeneous as in the glassy host medium, as evidenced by the similar peak heights in Fig. 7 for $L = 59$ and 99 .

Concerning the long-time dynamics, the non-Gaussian parameter also remains finite for the glassy host medium, and no important differences with the random configuration are observed. Therefore, contrary to what was previously pointed out [10], the non-Gaussianity observed at large length scales for the long-time dynamics in the inhomogeneous random host medium is also present in the homogeneous glassy one, and is not related to the presence of holes in the configuration of obstacles, the latter having effects only in the intermediate caging regime.

Another way of visualize the non-Gaussian effects at large length scales is obtained by representing the intermediate incoherent scattering function $F_s(q, t) = \langle \exp(-i\mathbf{q} \cdot \Delta \mathbf{r}(t)) \rangle$, at very long wavelengths $\lambda = 2\pi/q$. Brackets denote ensemble and angular average. Fig. 8 shows this latter function in the random host medium for $L = 99$ and $\rho = 6 \cdot 10^{-3}$, at different (long) wavelengths. (Note that the simulations have been extended one order of magnitude respect to those presented in Ref. [10].) The presence of non-Gaussian effects are made

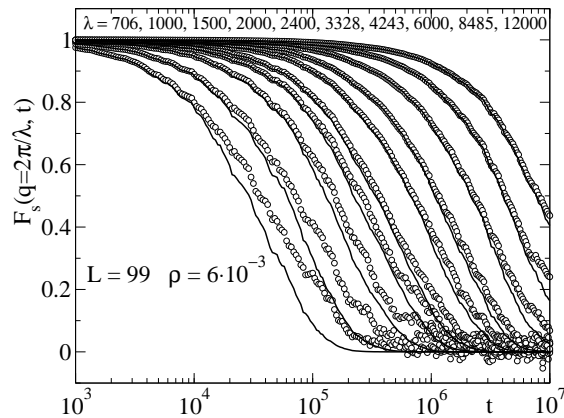


FIG. 8: Intermediate incoherent scattering function $F_s(q = 2\pi/\lambda, t)$ at different wavelengths λ for $\rho = 6 \cdot 10^{-3}$ and $L = 99$. Points correspond to simulation data in the random host medium. Lines are the curves in Gaussian approximation as calculated from the center-of-mass mean-squared displacement obtained from the simulation (see text).

clear by comparing the different curves with those corresponding to the Gaussian case in two-dimensions [25], $\exp[-\langle(\Delta r(t))^2\rangle q^2/4]$, where we use the center-of-mass mean-squared displacement $\langle(\Delta r(t))^2\rangle$ calculated from the simulations. From this comparison it is clear that significant non-Gaussian effects are still present at length scales of at least ~ 9000 , i.e. two orders of magnitude larger than the rod length. Whether this result indicates that the diffusion of a rod in a disordered array of obstacles is actually a Poisson process at any length scale is an open question.

VI. CONCLUSIONS

By means of molecular dynamics simulations, we have compared the dynamics of a rigid rod in two models of a 2d-disordered static host medium: a random configuration of soft disks and another “glassy” one obtained from freezing a liquid of soft disks in equilibrium. While the former is characterized by the presence of big holes and clusters of close obstacles, the latter presents an homogeneous structure. No significant differences have been observed in the translational dynamics of the rod center-of-mass. However, rotations are much more hindered in the glassy host medium.

Angular correlation functions have been calculated for a wide range of rod length and density of obstacles. In agreement with the predictions of the Mode Coupling Theory, these functions show a plateau at the time scale of the caging regime, and follow a time-length and a time-

density scaling for the long-time dynamics.

Strong non-Gaussian behavior has been observed at large length scales, though no significant differences are evidenced between the random and the glassy configuration of the obstacles. This result suggests that the long-time translational dynamics is not controlled by the presence of inhomogeneities in the host medium.

We thank E. Frey for useful discussions. A.J.M acknowledges a postdoctoral grant from the Basque Government. Part of this work was supported by the European Community’s Human Potential Program under contract HPRN-CT-2002-00307, DYGLAGEMEM.

-
- [1] H.A. Lorentz, Arch. Neerl. **10**, 336 (1905).
 - [2] C. Bruin, Phys. Rev. Lett. **29**, 1670 (1972).
 - [3] B.J. Alder and W.E. Alley, J. Stat. Phys. **19**, 341 (1978).
 - [4] W. Götze, E. Leutheusser and S. Yip, Phys. Rev. A **23**, 2634 (1981); *ibid.* **24**, 1008 (1981); *ibid.* **25**, 533 (1982).
 - [5] A. Masters and T. Keyes, Phys. Rev. A **26**, 2129 (1982).
 - [6] T. Keyes, Phys. Rev. A **28**, 2584 (1983).
 - [7] J. Machta and S.N. Moore, Phys. Rev. A **32**, 3164 (1985).
 - [8] P.M. Binder and D. Frenkel, Phys. Rev. A **42**, R2463 (1990).
 - [9] D.A. McQuarrie, *Statistical Physics* (University Science Books, Sausalito, CA, USA, 2000).
 - [10] A.J. Moreno and W. Kob, Philos. Magaz. B (to be published); cond-mat/0303510.
 - [11] W. Kob, and H.C. Andersen, Phys. Rev. E **51**, 4626 (1995).
 - [12] F. Sciortino, P. Gallo, P. Tartaglia and S.H. Chen, Phys. Rev. E **54**, 6331 (1996).
 - [13] S. Mossa, R. di Leonardo, G. Ruocco and M. Sampoli, Phys. Rev. E **62**, 612 (2000).
 - [14] D. Caprion and H.R. Schober, Phys. Rev. B, **62**, 3709 (2000).
 - [15] J. Colmenero, F. Alvarez and A. Arbe, Phys. Rev. E **65**, 041804 (2002).
 - [16] W. van Meegen, J. Phys.: Condens. Matter **14**, 7699 (2002).
 - [17] E.R. Weeks, and D.A. Weitz, Chem. Phys. **284**, 361 (2002).
 - [18] A.M. Puertas, M. Fuchs, and M.E. Cates, Phys. Rev. E **67**, 031406 (2003).
 - [19] U. Bengtzelius, W. Götze and A. Sjölander, J. Phys. C **17**, 5915 (1984).
 - [20] E. Leutheusser, Phys. Rev. A **29**, 2765 (1984).
 - [21] W. Götze and L. Sjögren, Rep. Prog. Phys. **55**, 241 (1992).
 - [22] W. Götze, J. Phys.: Condens. Matter **11**, A1 (1999).
 - [23] F. Affouard and M. Descamps, Phys. Rev. Lett. **87**, 035501 (2001).
 - [24] J.C. Phillips, Rep. Prog. Phys. **59**, 1133 (1996).
 - [25] J.P. Hansen and I.R. McDonald., *Theory of Simple Liquids*, (Academic Press London, 1986).